

# A Theoretical Investigation of the Electronic Structure and Spectrum for $S_3^-$

Helge Johansen

Chemistry Department B, DTU 207, Technical University of Denmark, DK-2800 Lyngby, Denmark

Johansen, H., 1995. A Theoretical Investigation of the Electronic Structure and Spectrum for  $S_3^-$ . – Acta Chem. Scand. 49: 79–84 © Acta Chemica Scandinavica 1995.

Multi-configurational electron correlation methods have been used to analyze the electronic structure and spectrum for  $S_3^-$ , the chromophore in lapis lazuli and ultramarine. The broad peak in the visible part of the spectrum is assigned to two electronic transitions, in accord with fairly recent MCD measurements. Also the reported UV transition fits well with the present calculations. Basis sets including *f*-functions are used in MCSCF calculations with more than  $10^5$  configurations followed by a second-order perturbation treatment. The electron density as well as the spin density are analyzed on a somewhat lower level of accuracy, and they show no surprising features. The spin density resembles very much the electron density for the singly occupied  $\pi^*$ -orbital.

The beautiful colour of the gem lapis lazuli and the pigment in ultramarine is due to the ion  $S_3^-$  trapped in a sodalite cage.<sup>1,2</sup> The colour is caused by a broad absorption around 620 nm followed by a region with no absorption down to 350 nm.<sup>3–5</sup> The visual appearance gives association to transition-metal atoms rather than to sulfur. This is intriguing, and one of the reasons for undertaking the present study.

$S_3^-$  has an unpaired electron in a  $\pi^*$ -orbital. Its valence isoelectronic analog one row above in the periodic system is  $O_3^-$ , the ozonide ion, and like this it is bent with an angle of about  $115^\circ$ . The absorption spectrum of  $O_3^-$  has a broad peak around 430 nm followed by low absorption down to 240 nm;<sup>6</sup> the two spectra thus show similarities, but as one might expect, the transitions are found at lower wavelengths for  $O_3^-$ . Neither of the recorded experimental absorption spectra shows any splitting of the outer band, with the possible exception of the spectrum published by Holzer *et al.*<sup>3</sup> of  $S_3^-$ , where a small shoulder is shown. The magnetic circular dichroism spectrum of  $S_3^-$ ,<sup>5</sup> however, indicates the possibility of two transitions in this region, and so does a photodissociation study of  $O_3^-$ .<sup>7</sup> It is therefore of interest whether a theoretical investigation will show one or two transitions, and if  $O_3^-$  and  $S_3^-$  are different on this point.

Since  $S_3^-$  is a naturally occurring simple and stable radical, it is also of interest to investigate the electronic structure of the system in terms of electron density, the Laplacian of the density, and the spin density.  $S_3^-$  has been the target of previous calculations: SW-SCF- $X\alpha$  by Cotton *et al.*<sup>8</sup> and *ab initio* calculations by Hinchliffe<sup>9</sup> and Bash.<sup>10</sup> There have been a number of investigations on

$O_3^-$ , and only a recent and accurate study by González-Luque *et al.*<sup>11</sup> will therefore be mentioned in this connection, both for its results and as an entry to the literature.

## Geometry

The  $S_3^-$  ion in its ground state has a bent structure, as found in both theoretical and experimental studies, and does not form a ring. The aim of the present investigation is not geometry optimization as such: the attention is on the electronic structure of the ground state and on the vertical excitation energies. The involved electronic states have, of course, differences in geometry, and vibrational levels as well as the effects of the surroundings would have to be considered explicitly, if the aim were more than an assignment of the spectrum.

The geometry adopted for all the calculations on  $S_3^-$  was (200 pm;  $115^\circ$ ), where the numbers (*a* pm; *b*°) signify that the X–X distance is *a* pm and the X–X–X angle is *b* degrees, with X being S or O. Using Gaussian 90<sup>12</sup> and 6-31G\* basis functions resulted in (199 pm;  $115.0^\circ$ ) on the UHF (unrestricted Hartree–Fock) level and (201 pm;  $115.5^\circ$ ) using the MP2 (Møller–Plesset second-order perturbation) approach.<sup>13</sup> Hinchliffe<sup>9</sup> found (200 pm;  $113^\circ$ ) from Hartree–Fock calculations and Bash<sup>10</sup> (208 pm;  $115.9^\circ$ ) using MC SCF (multi-configurational self-consistent field). There does not seem to be any accurate experimental determination of the structure.

For  $O_3^-$  the UHF 6-31G\* results are (131 pm;  $116.0^\circ$ ), the corresponding MP2 values (134 pm;  $114.8^\circ$ ),<sup>13</sup> and

two more accurate calculations find (136.1 pm; 115.4°)<sup>11</sup> and (139 pm; 115.3°),<sup>10</sup> respectively. The experimental values for the crystals of RbO<sub>3</sub> and KO<sub>3</sub><sup>14</sup> are [134.1(15) pm; 114.6(13)°] and [135.7(5) pm; 113.4(8)°], where also the uncertainties have been listed. A gas-phase investigation<sup>15</sup> finds [134(3) pm; 113(2)°]. The calculated values for O<sub>3</sub><sup>-</sup> agree well with the experimentally determined results, and there is therefore good reason to believe that the adopted S<sub>3</sub><sup>-</sup> geometry will be sufficiently accurate. In order to evaluate the uncertainties in the S<sub>3</sub><sup>-</sup> calculations reported below, some parallel calculations have been undertaken for O<sub>3</sub><sup>-</sup>, and the geometry chosen for these was (134.9 pm; 114°), which is an average of the experimental values for RbO<sub>3</sub> and KO<sub>3</sub>.

All calculations have been performed in C<sub>2v</sub> symmetry with C<sub>2</sub> along the z-axis and the three atoms in the yz-plane. The π\*-orbital with the unpaired electron has, therefore, b<sub>1</sub> symmetry, and transforms as x in this coordinate system. The ground state of the ion is accordingly <sup>2</sup>B<sub>1</sub>. It should be noted that some investigations use a different notation.

### Details of calculations

Two different basis sets have been used in the S<sub>3</sub><sup>-</sup> calculations: A primitive (12s, 9p, 1d) set contracted as [7s, 5p, 1d] in a segmented contraction, and a primitive (17s, 12p, 5d, 4f) set contracted as [5s, 4p, 3d, 1f] in a general contraction. The basis sets will be denoted B1 and B2, respectively, in the following. B1 is due to Veillard<sup>16</sup> but augmented with a set of d functions.<sup>17</sup> B2 is a generally contracted basis set of the atomic natural orbital (ANO) type<sup>18</sup> reported by Widmark *et al.*<sup>19</sup> For the comparative calculations on O<sub>3</sub><sup>-</sup> a generally contracted (14s, 9p, 4d, 3f)/[4s, 3p, 2d, 1f] ANO basis set was used.<sup>20</sup>

The applied methods were restricted Hartree–Fock (RHF), unrestricted Hartree–Fock (UHF), complete-active-space multi-configurational self-consistent field (CASSCF)<sup>21</sup> and CASPT2.<sup>22,23</sup> The last of these methods is a Møller–Plesset-type perturbation theory to second order, where the zeroth-order Hamiltonian is defined as a Fock-type one-electron operator. In some of the calculations, only the diagonal part of the Fock matrix is included (termed PT2D), since the use of the full matrix (PT2F) gives changes, which are relatively insignificant compared to other errors in the investigation.

The CASPT2 and most of the CASSCF calculations were performed using the program system MOLCAS-2,<sup>24</sup> whereas the other calculations were performed using local programs and adaptations.

### The electronic structure of the ground state

The ground state of S<sub>3</sub><sup>-</sup> has <sup>2</sup>B<sub>1</sub> symmetry with a singly occupied π\*(b<sub>1</sub>) orbital in the RHF description. The total

density and the Laplacian of the density are shown in Fig. 1, where also the Bader-type<sup>25</sup> partitioning of the ion has been indicated. The basis set used for displaying densities was B1 throughout, and no great changes are expected with B2. On the RHF level the two outer S atoms carry a charge of -0.55 each, leaving the atom in the middle with a positive charge of 0.10 using a Mulliken population analysis.<sup>26</sup> The overlap population between bonding atoms is 0.28, a fairly low figure, which is due to the electronically crowdedness of the system as well as the antibonding orbital. For comparison, the largest of the CASSCF calculations results in charges of -0.49 for the outer atoms and -0.03 for the atom in the middle.

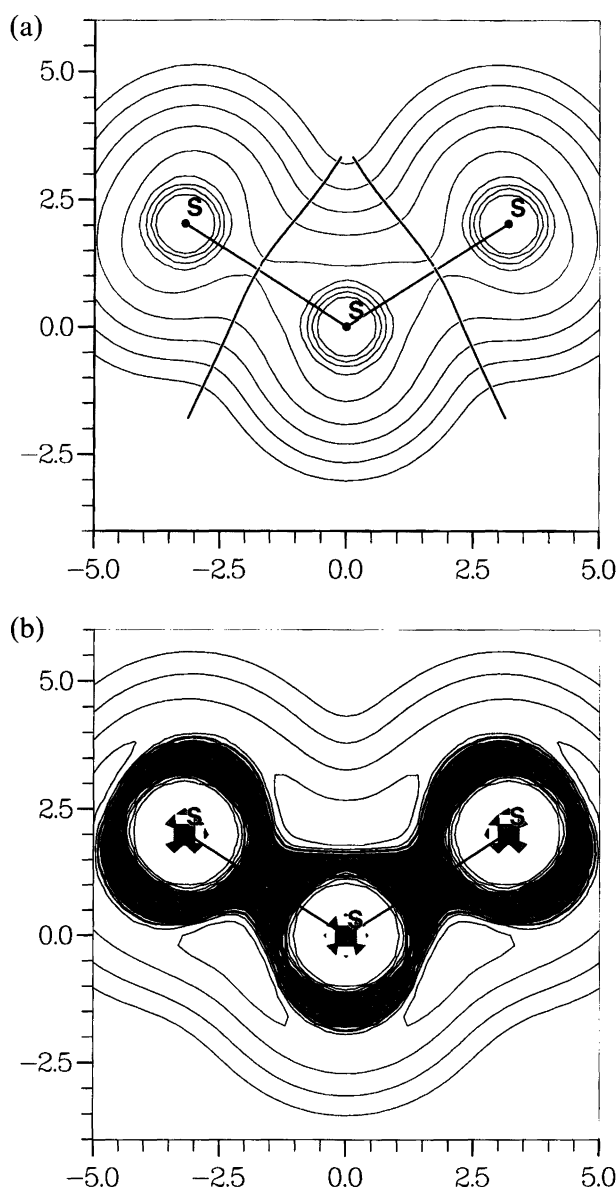


Fig. 1. (a) Total RHF density in the molecular plane for S<sub>3</sub><sup>-</sup> with atomic regions separated by Bader lines; contours from 0.01 to 2.56  $ea_0^{-3}$  with a factor two between adjacent levels. (b) Laplacian of the density; negative regions indicated with grey.

The Laplacian of the density, apart from the shell structure of the atoms, shows the concentrations of density along the bonds, in particular close to the center atom, and concentrations in lone-pair regions.

A difference density between  $S_3^-$  and  $S_3$  in a plane  $1a_0$  above the plane of the molecule ( $1a_0 = 52.92$  pm) and at the RHF level of approximation shows features which are almost identical to the density of the singly occupied  $\pi^*$ -orbital (Fig. 2). The spin density of the system is, of course, dominated by the features of the singly occupied orbital, but the RHF level by nature can show only fea-

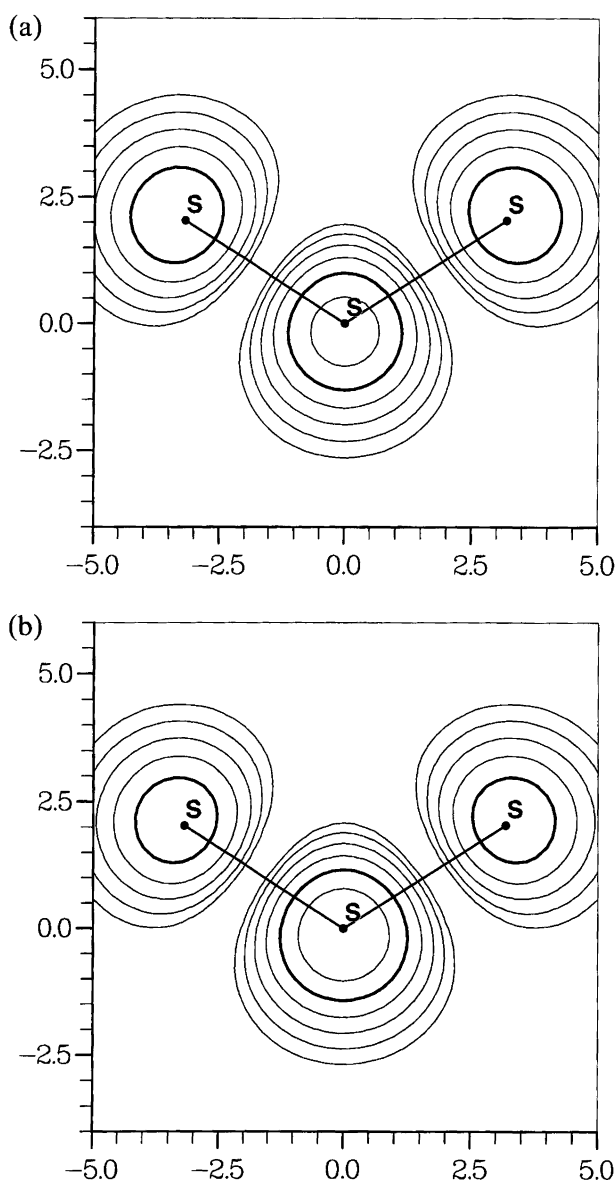


Fig. 2. (a) Difference density at the RHF level between  $S_3^-$  and  $S_3$  in a plane  $1a_0$  above the molecular plane; contours from  $0.000625$  to  $0.02 ea_0^{-3}$  with a factor two between adjacent levels, the  $0.01$  contour has been drawn with a thick line. (b) Density for the  $\pi^*$ -orbital of  $S_3^-$  at the RHF level.

tures of either  $\alpha$  or  $\beta$  spin, and the investigation was therefore extended to the UHF and CASSCF methods, in order to get a more detailed analysis (Fig. 3).

The  $\pi^*$ -orbital, apart from its nodes on the bonds, has a node in the molecular plane, and spin density features in this plane must therefore have their origin elsewhere. The plane of the molecule and a plane  $1a_0$  above have been depicted. Negative features show up on the bonds in the CASSCF results, but they are small, and the general picture does not deviate much from the electron density of the  $\pi^*$ -orbital. There are also some small features in the plane of the molecule for the CASSCF spin density, which add majority spin to the central atom and negative density to the bond and to the far side of the outer atoms. The CASSCF calculations in this case distribute nine electrons in nine active orbitals, with each symmetry contributing two orbitals, apart from  $b_1$ , which supplies three active orbitals. The UHF calculations show similar but exaggerated trends. This has been seen before,<sup>27</sup> and even though a recent investigation<sup>28</sup> concludes that the negative features in UHF spin densities are due to spin contamination from higher spin states, the unprojected UHF results often show good qualitative agreement with multiconfigurational SCF results. The value for  $\langle S^2 \rangle$  in the present UHF calculation is  $0.767$ , which is not very far from  $0.75$ , the value for a pure doublet.

As seen in Fig. 3, the spin density is highest on the central atom, and a spin population analysis of the most accurate CASSCF calculation using basis set B2 results in  $0.43$  for the central atom and  $0.29$  for each of the other two. This distribution is opposite that of the total density, which has the highest population on the outer atoms in order to reduce repulsion in this electron-rich negative ion.

Table 1. Total energy for the  ${}^2B_1$  ground state of  $S_3^-$  as a function of basis set, method and size of the active space.

Calculation	Energy <sup>a</sup>
Basis set B1	
RHF	-1192.6018
UHF	-1192.6070
CASSCF 9/9	-1192.6696
Basis set B2	
RHF	-1192.696045
CASSCF 9/9	-1192.770195
CASSCF 13/11	-1192.784066
CASSCF 17/13	-1192.791236
PT2D 9/9	-1193.297692
PT2F 9/9	-1193.300928
PT2D 13/11	-1193.301659
PT2F 13/11	-1193.305374
PT2D 17/13	-1193.307612
PT2F 17/13	-1193.307089

<sup>a</sup> In atomic units, au;  $1 \text{ au} = 4.35975 \times 10^{-18} \text{ J}$ .

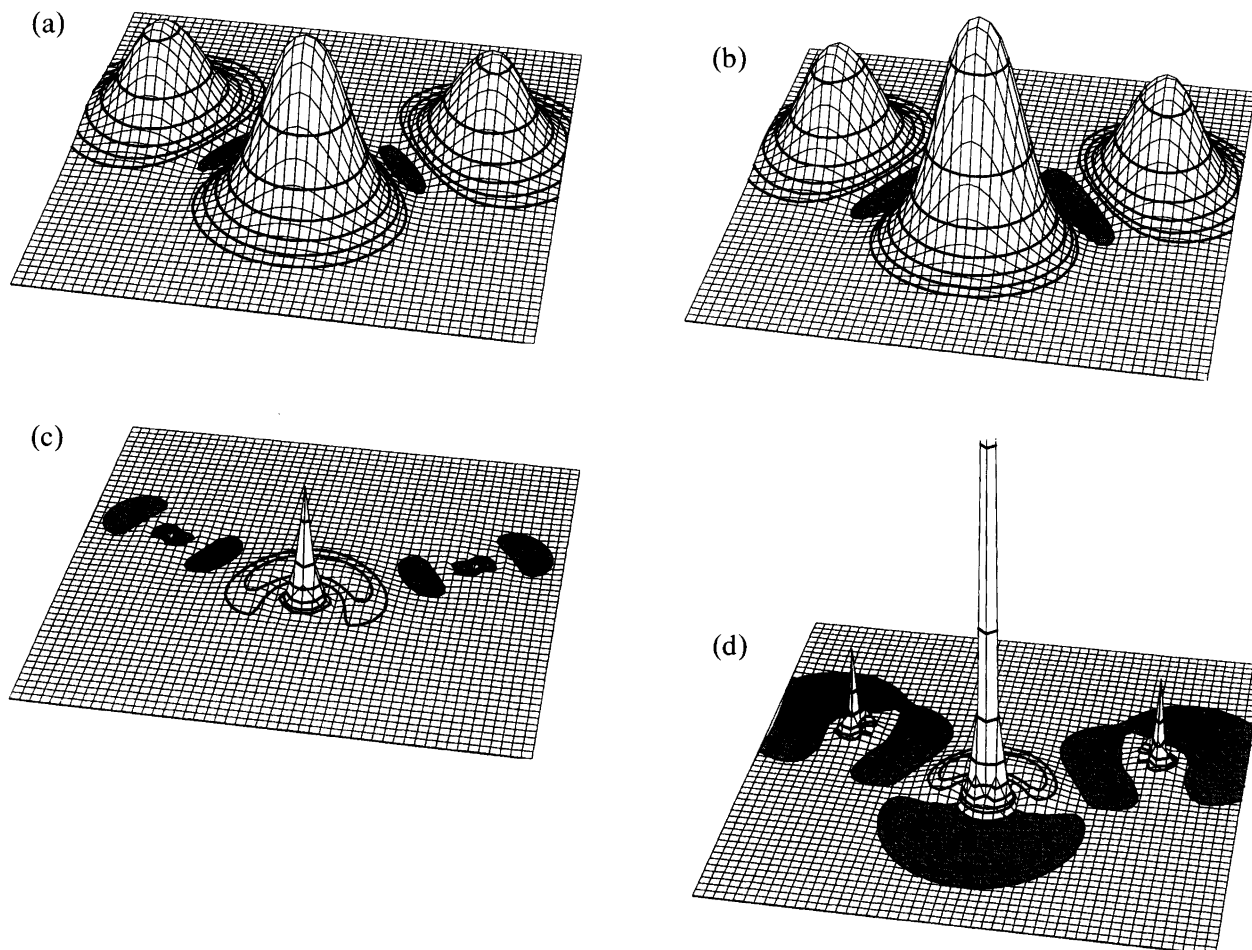


Fig. 3. (a) CASSCF spin density for  $S_3^-$  using basis set B1 and the 9/9 space for a plane  $1a_0$  above the molecular plane; contours start at  $\pm 0.000625 ea_0^{-3}$ , negative regions are indicated with grey, and there is a factor two between adjacent levels. (b) UHF spin density  $1a_0$  above the molecular plane. (c) CASSCF spin density in the plane of the molecule. (d) UHF spin density in the plane of the molecule.

### The electronic spectrum

The absorption spectrum of  $S_3^-$  shows a pronounced peak around 620 nm followed by a region with low absorption down to 350 nm, and a second absorption band at 275 nm.<sup>3-5</sup> The MCD spectrum<sup>5</sup> indicates two transitions under the broad absorption band, and it is therefore the aim to interpret these spectra and assign the bands.

Table 2. Vertical excitation energies in eV ( $1 \text{ eV} = 1.60219 \times 10^{-19} \text{ J}$ ) for  $S_3^-$  from CASSCF calculations with basis set B2.

Excited state	CAS 9/9	CAS 13/11	CAS 17/13	Exp. <sup>a</sup>
$1^2A_1$	3.29	1.94	1.78	1.91
$1^2A_2$	2.41	2.23	2.18	2.36
$2^2B_1$	5.09	4.93	4.90	4.51
$1^2B_2$	2.36	1.85	1.72	No <sup>b</sup>

<sup>a</sup> Ref. 5. <sup>b</sup> Not allowed.

The total energy for the  $^2B_1$  ground state with the applied basis sets and methods have been listed in Table 1. From  $O_3^-$  it is known<sup>11</sup> that correlation plays an important role, and that multi-reference functions are necessary to describe properly both the dynamic and the static parts of the correlation energy. The strategy in selecting the active space has been to include at least one of the doubly occupied and one of the unoccupied orbitals (in the RHF sense) from each symmetry, together with the singly occupied  $b_1$  orbital. The simplest space of this kind has nine active electrons in nine active orbitals leading to about 2200 configuration state functions (CAS 9/9) of each symmetry. The space is then extended with doubly occupied orbitals to 13/11 and 17/13. The latter space consists of a little more than  $10^5$  configurations and includes all valence electrons from sulfur 3s and 3p, apart from two electrons corresponding to the lowest valence orbital, which has  $a_1$  symmetry.

The results of the calculations show a reasonable convergence with the extension of the active space (Tables 2 and 3), and they compare well with experimental results,

**Table 3.** Vertical excitation energies in eV for  $S_3^-$  from CASPT2 calculations based upon the CASSCF calculations of Table 2 (experimental values given in Table 2).

Excited state	PT2D 9/9	PT2D 13/11	PT2F 13/11	PT2D 17/13	PT2F 17/13
$1^2A_1$	2.61	1.82	1.74	1.81	1.77
$1^2A_2$	2.25	2.06	1.98	2.01	1.98
$2^2B_1$	4.68	4.47	4.50	4.42	4.45
$1^2B_2$	1.74	1.61	1.68	1.75	1.70

in particular the largest active spaces and at the CASPT2 level. Only the 9/9 calculations of the  $^2A_1$  excitation energy breaks the pattern: the rest of the results show good stability.

The CASSCF results for the  $2^2B_1$  state correspond to the second root of  $b_1$  symmetry optimized for the  $1^2B_1$  ground state. The CASPT2 calculations on the  $2^2B_1$  state are performed accordingly. This may be a somewhat questionable approach, in particular for the CASPT2 calculations, but with the great stability of the results it may be justifiable. Second roots corresponding to the other  $C_{2v}$  symmetries are found at higher energies than  $2^2B_1$ .

The assignment is therefore that the outer band corresponds to two transitions,  $^2A_1$  and  $^2A_2$ , with a preference of  $^2A_1$  being at the longest wavelength. The same order appears from the calculations by Bash.<sup>10</sup> The peak at 275 nm (4.51 eV) is assigned to a transition to the  $2^2B_1$  state, and it is assumed that the  $^2B_2$  state does not show up in the spectrum, since it is not electric dipole allowed. The  $^2B_2$  state would have been predicted to be close to or at slightly longer wavelengths than the  $^2A_1$  transition.

Even though this assignment of the spectrum looks fairly convincing, it should be borne in mind that it is based upon vertical transitions, and that no attention has been given to the vibrations. The effects of the surroundings have not been treated either, and these may be substantial for an electron-rich system carrying a negative charge. The results should therefore only be considered for their qualitative virtues, even though powerful basis sets and large configuration expansions have been used.

In order to have a handle on the accuracy of the results, some calculations have been repeated for  $O_3^-$  (Table 4). CASSCF has been applied with the 17/13 space, and a CASPT2D has been performed on top of this. The results for  $O_3^-$  are very similar to those for  $S_3^-$ ,

**Table 4.** Vertical excitation energies in eV for  $O_3^-$ .<sup>a</sup>

Excited state	CAS 17/13	PT2D 17/13	Exp.
$1^2A_1$	2.29	2.35	2.05 <sup>b</sup>
$1^2A_2$	3.09	2.62	2.65 <sup>b</sup>
$2^2B_1$	7.46	6.85	> 5 <sup>c</sup>
$1^2B_2$	2.14	2.18	No <sup>d</sup>

<sup>a</sup> The corresponding total energies for the  $^2B_1$  ground state are  $-224.641128$  au and  $-255.203889$  au for the CASSCF and PT2D calculations, respectively. <sup>b</sup> Ref. 7, with the assignment of the two states reversed. <sup>c</sup> Ref. 6, where the main absorption band has its maximum at 2.88 eV. <sup>d</sup> Not allowed.

there is just a shift to somewhat higher excitation energies, as expected. Two transitions are found under the main absorption band, and the agreement with experimental results is absolutely acceptable, considering the inadequacies of the present approach as described above. It should, however, be noted that the experimental assignments of the two outer transitions have been reversed in Table 4, in order to match the calculated numbers.

## Conclusions

For both  $S_3^-$  and  $O_3^-$  the broad peak in the absorption spectrum (located around 620 nm for  $S_3^-$  and 430 nm for  $O_3^-$ ) is assigned to two transitions. The terms involved are  $^2A_1$  and  $^2A_2$  with transitions to  $^2A_1$  calculated at the longest wavelength in both cases. The experimental investigation on  $O_3^-$  based upon laser photodissociation<sup>7</sup> favours the reverse assignment with  $^2A_2$  at the longest wavelengths. Their argument for this does not seem to be very strong (and the order has tentatively been changed in Table 4), but the results of the present calculations are not sufficiently accurate to make a definite conclusion on this point.

For both ions, the stretch with low absorption is confirmed, and for  $S_3^-$  the peak at 275 nm, corresponding to 4.51 eV, is assigned to the  $2^2B_1$  state, which is found at 4.45 eV in the most elaborate calculation (CASPT2F 17/13).

The electron density, the Laplacian of the density, and the spin density show features with no major surprises. The outer atoms carry most of the negative charge, and this is a contrast to the spin density, in which the central atom shows the highest peak. The spin density as such is very similar to the electron distribution for the singly occupied  $\pi^*$ -orbital. Only minor regions with negative spin density are found.

**Acknowledgements.** S. E. Harnung is acknowledged for discussions leading to the present study, and K. Møller for doing preliminary geometry optimizations on the systems. The work was supported by The Danish Natural Science Research Council.

## References

1. Seel, F. and Güttler, H.-J. *Angew. Chem.* 85 (1973) 416.
2. Chivers, T. *Nature (London)* 252 (1974) 32.

3. Holzer, W., Murphy, W. F. and Bernstein, H. J. *J. Mol. Spectrosc.* 32 (1969) 13.
4. Chivers, T. and Drummond, I. *Inorg. Chem.* 11 (1972) 2525.
5. Bang, E. and Harnung, S. E. *Dansk Kemi* 72 (1991) 460.
6. Sehested, K., Holcman, J., Bjergbakke, E. and Hart, E. J. *J. Phys. Chem.* 86 (1982) 2066.
7. Hiller, J. F. and Vestal, M. L. *J. Chem. Phys.* 74 (1981) 6096.
8. Cotton, F. A., Harmon, J. B. and Hedges, R. M. *J. Am. Chem. Soc.* 98 (1976) 1417.
9. Hinchliffe, A. *J. Mol. Struct. (THEOCHEM)* 85 (1981) 207.
10. Basch, H. *Chem. Phys. Lett.* 157 (1989) 129.
11. González-Luque, R., Merchán, M., Borowski, P. and Roos, B. O. *Theor. Chim. Acta* 86 (1993) 467.
12. Nobes, R. *Gaussian 90 for Fujitsu FACOM Computers*, Australian National University Supercomputer Facility, Canberra, Australia 1990.
13. Møller, K., Technical University of Denmark, Lyngby, Denmark. *Personal communication*.
14. Schnick, W. and Jansen, M. *Angew. Chem.* 97 (1985) 48.
15. Wang, L. J., Woo, S. B. and Helmy, E. M. *Phys. Rev. A* 35 (1987) 759.
16. Veillard, A. *Theor. Chim. Acta* 12 (1968) 405.
17. Roos, B. and Siegbahn, P. *Theor. Chim. Acta* 17 (1970) 199.
18. Almlöf, J. and Taylor, P. R. *J. Chem. Phys.* 86 (1987) 4070.
19. Widmark, P.-O., Persson, B. J. and Roos, B. O. *Theor. Chim. Acta* 79 (1991) 419.
20. Widmark, P.-O., Malmqvist, P.-Å. and Roos, B. O. *Theor. Chim. Acta* 77 (1990) 291.
21. Roos, B. O., Taylor, P. R. and Siegbahn, P. E. M. *Chem. Phys.* 48 (1980) 157.
22. Andersson, K., Malmqvist, P.-Å., Roos, B. O., Sadlej, A. J. and Wolinski, K. *J. Phys. Chem.* 94 (1990) 5483.
23. Andersson, K., Malmqvist, P.-Å. and Roos, B. O. *J. Chem. Phys.* 96 (1992) 1218.
24. MOLCAS version 2; Andersson, K., Fülcher, M. P., Lindh, R., Malmqvist, P.-Å., Olsen, J., Roos, B. O. and Sadlej, A. J., University of Lund, Sweden, and Widmark, P.-O., IBM, Sweden 1991.
25. Bader, R. F. W. *Chem. Rev.* 91 (1991) 893.
26. Mulliken, R. S. *J. Chem. Phys.* 23 (1955) 1833.
27. Johansen, H. and Andersen, N. K. *Mol. Phys.* 58 (1986) 965.
28. Cassam-Chenaï, P. and Chandler, G. S. *Int. J. Quantum Chem.* 46 (1993) 593.

Received March 23, 1994.